Journal of Sound and Vibration 617 (2025) 119292

Contents lists available at ScienceDirect

Journal of Sound and Vibration

journal homepage: www.elsevier.com/locate/jsvi

Mode veering via inertial coupling

Andrew Jacques *, Sondipon Adhikari

James Watt School of Engineering, The University of Glasgow, Glasgow, Scotland, United Kingdom

ARTICLE INFO

Keywords:
Inertial amplifier
Inertial coupling
Mode veering
Eigenvalue veering

ABSTRACT

Mode veering, a phenomenon where natural frequencies of adjacent modes converge and then diverge while exchanging modal characteristics, is critical for designing dynamic systems and predicting structural behaviour. While extensively studied in stiffness-coupled systems, the impact of inertial coupling, particularly through inertial amplifiers, on mode veering remains unexplored despite their growing applications in vibration control and energy harvesting. This paper presents the first mathematical demonstration of mode veering induced by inertial coupling in a coupled double oscillator system. Through rigorous eigenvalue analysis and hyperbolic transformation, it is proven that mode veering invariably occurs in systems with pure inertial coupling or any combination of inertial and stiffness coupling, with one notable exception that occurs at the system's point of symmetry. This exception is particularly significant as it enables strong mode veering effects even at high coupling stiffness, a characteristic previously unattainable in traditional stiffness-coupled systems. By identifying the system's symmetry point and establishing its relationship to eigenvalue behaviour, a rigorous framework for understanding and predicting mode veering in combined coupling systems is provided. These findings not only expand the theoretical understanding of mode veering but also offer new possibilities for frequency control in multi-degree-of-freedom systems, particularly relevant for vibration control, and energy harvesting applications where traditional stiffness-based approaches may be limiting.

1. Introduction

Mode veering, or eigenvalue veering, can occur in coupled systems and can be identified by the eigenvalues of two or more modes converging towards and then diverging away from each other as a system variable is changed along a range of potential values [1–3]. This behaviour is accompanied by a shift in both the eigenvalue and eigenvector behaviours where the modes seemingly swap their responses to a changing system [4–6]. This effect is usually strongest for weakly coupled systems [7,8] one where, for stiffness coupling, the coupling element has low stiffness. Mode veering is usually of particular importance during the design phase of a system when variables are most prone to significant changes and must be monitored or otherwise accounted for to avoid sudden or unexpected changes in the eigenvalues of different modes [9–11]. It can also be important in vibrating systems where the loading can be expected to change during use [12–15] and can be of particular importance during the maintenance of existing structures when vibration control systems might need to be retuned as changes in the structural shape and material properties due to age can induce mode veering [16,17].

While mode veering is generally described and explored in the context of structures where stiffness coupling is the mechanism which induces the veering effect, there are other potential coupling mechanisms. Gyroscopic coupling has been described in rotating

* Corresponding author.
E-mail addresses: a.jacques.1@research.gla.ac.uk (A. Jacques), Sondipon.Adhikari@glasgow.ac.uk (S. Adhikari).

https://doi.org/10.1016/j.jsv.2025.119292
Received 22 January 2025; Received in revised form 4 June 2025; Accepted 6 June 2025

Available online 26 June 2025

bodies under external forces, such as spin stabilised satellites [18], and due to aerodynamic forces on very small systems [19]. Inertial coupling can be utilised to interpret the behaviour of porous mediums such as sands and soils [20], to describe the behaviour of particles within certain types of fluid flows [21,22], to describe the boundary layer behaviour of two fluid flows of markedly different properties [23,24] as well as to model the aeroelastic galloping behaviour of small cross-sectioned structural bodies in crosswind conditions [25]. Of these varied coupling mechanisms, the existence of mode veering can be considered well established for stiffness coupling scenarios but has also been described in gyroscopic coupling as well [26]. Due to both the past use of inertial coupling for modelling fluid particle interactions as well as the relative lack of documentation on mode veering in inertial coupling systems the growing interest in inertial amplifiers in structural mechanics therefore presents a potential gap in the existing knowledge surrounding their dynamic behaviour where multi-degree of freedom systems and their potential for inertial coupling and possible mode veering are concerned

There is a growing body of research into Inertial Amplifiers [27] with particular focus on proposed uses in mechanical systems [28] and meta-materials [29–31]. Inertial Amplifiers are also being investigated for their potential to open up new avenues for energy harvesting [32–34] as well as their promising attributes for frequency control [35,36]. Current investigations in the literature have proposed applications in single degree of freedom systems [37] or in systems where only a single oscillator is directly influenced by the inclusion of an inertial amplifier [38]. In addition to these cases, inertial amplifiers are also being regarded for applications in multi-degree of freedom systems where several oscillators can be simultaneously affected by the inclusion of an inertial amplifier in between them [39–41]. The primary interest in inertial amplifiers for the proposed applications is their potential for including additional tools for frequency control [42–44], particularly in the ability of inertial amplifiers to induce a shift in the natural frequencies of the connected oscillators [45]. However, the possible effects of inertial amplifier inclusion into such multi-degree of freedom systems and their multi-modal frequency behaviour, particularly the potential for mode veering which can occur in such coupled oscillator systems remains under studied. This paper seeks to fill in this gap that has been identified by demonstrating that mode veering occurs for inertially coupled systems and shows that the mode veering behaviour due to stiffness or inertial coupling are specific forms of a more general coupling behaviour that is likewise identified and described in this paper.

In this paper, a coupled double oscillator system is considered, where a simple inertial amplifier is included between the two oscillators both alongside and instead of a coupling spring. A coupled double oscillator was selected as its dynamic system can be regarded as a common base unit used in the approximations of a large variety of mechanical systems [46]. It is also used to describe the unit cells [47] used to build many larger types of multi-degree of freedom dynamic systems [48], especially when linked up in series [49,50]. A coupled double oscillator can also be used to analyse the two specific modes involved in a mode veering phenomenon for a larger system without having to calculate the other uninvolved modes that are not of interest. In addition, its dynamic behaviour is well studied [51] and so gives a useful comparison for potential systems utilising inertial coupling.

This paper is laid out as follows; in Section 2, the system model is introduced. Using the Lagrange Method for determining the energy balance of the mass and stiffness normalised system, the mass and stiffness matrices are obtained and the Euler–Lagrange equations are used to obtain the equations of motion for the generalised system. It is demonstrated that any combination of coupling inertial amplifier masses or coupling springs can be reduced to two distinct variables in the equations. In Section 3 the mass and stiffness matrices are used to obtain the frequency equation and the generalised values of the eigenvalues for a coupled double oscillator with both a coupling spring and coupling inertial amplifier of any form or type. The eigenvalues for a pure inertial amplifier coupling are shown to be always distinct. In Section 4 the co-ordinate translation and reference frame rotation hyperbolic method developed to demonstrate mode veering in all pure stiffness coupling double oscillator systems [51] is used to demonstrate that for a generalised case, both for varying stiffness and varying mass, that mode veering will likewise always occur in all pure inertial coupling double oscillator systems. It is demonstrated that the same holds true for almost all systems with any form of combined coupling, as well as highlighting the one exception case. In Section 5 is a comparison of the inverse symmetries present in both pure stiffness coupling and pure inertial coupling as well as how they relate to the more general combined coupling case. The point at which a coupled double oscillator would have complete symmetry and thus have non-distinct eigenvalues is identified and it is demonstrated how this point of symmetry is integral to describing the behaviour of eigenvalue loci curves. Graphical demonstrations of double oscillator systems with a combination of stiffness and inertial coupling are included in Section 6 and the difference in dynamic behaviour between pure stiffness, pure inertial and combined cases are discussed. Conclusions are drawn in Section 7.

2. System model and the equations of motion

Consider a classic coupled double oscillator suspended by a pair of fixed springs, one for each mass, and then include a stiffened simple inertial amplifier between the two masses alongside the coupling spring. This inertial amplifier consists of two small masses, each connected to the primary masses by a pair of hinged rods and to each other by a spring [27]. This system, Fig. 1 would then contain four masses, with both of the inertial amplifier masses being of equal magnitude; m_1, m_2 and m_a as well as four springs; k_1, k_2, k_3 and k_4. If the system is mass and stiffness-normalised, then each variable can be written as a ratio with respect to m_1 or k_1:

$$m_1 = m, \qquad m_2 = \gamma m, \qquad m_a = \mu m, \qquad k_1 = k, \qquad k_2 = \beta k, \qquad k_3 = \alpha k \qquad \text{and} \qquad k_4 = \eta k$$

where $\alpha, \beta, \gamma, \eta, \mu$ are the ratios of the normalised variables. Using the Lagrange Method for determining the energy balance of the system:

$$L = T_{\text{total}} - U_{\text{total}} \tag{1}$$

where L is the total energy of the system, T_{total} is the kinetic energy of the system and U_{total} is the potential energy of the system. For the system outlined in Fig. 1, the kinetic energies are as follows:

$$T_{m1} = \frac{1}{2}m\dot{y}_1^2, \qquad T_{m2} = \frac{1}{2}\gamma m\dot{y}_2^2, \qquad T_u = \frac{1}{2}\mu m\dot{u}^2 \qquad \text{and} \qquad T_v = \frac{1}{2}\mu m\dot{v}^2 \tag{2}$$

where T_{m1} defines the kinetic energy of the mass m_1, T_{m2} defines the kinetic energy of the mass m_2 and $T_{u,v}$ defines the kinetic energies of each amplifier mass in the perpendicular and parallel displacement directions respectively. While $\dot{y}_{1,2}$ is the axial velocity of each oscillator mass, $y_{1,2}$ is the axial displacement of each oscillator mass while u and v are, respectively, the axial and perpendicular displacements of each amplifier mass. As u and v apply equally to each of the amplifier masses then their total displacement kinetic energy, T_{ma}, can be written as follows:

$$T_{ma} = T_u + T_v = \frac{1}{2}\mu m(\dot{u}^2 + \dot{v}^2) \tag{3}$$

In addition, the potential energies of the system are:

$$U_{k1} = \frac{1}{2}ky_1^2, \qquad U_{k2} = \frac{1}{2}\beta k(y_2 - y_1)^2, \qquad U_{k3} = \frac{1}{2}\alpha k y_2^2, \qquad \text{and} \qquad U_{k4} = \frac{1}{2}\eta k(2u)^2 \tag{4}$$

where U_{k1} defines the potential energy of the spring k_1, U_{k2} defines the potential energy of the spring k_2, U_{k3} defines the potential energy of the spring k_3 and U_{k4} defines the potential energy of the spring k_4. Because the inertial amplifier is composed of small masses suspended by rigid rods, the kinematic relations of rigid rods can be applied:

$$v\cos\phi = u\sin\phi \tag{5}$$

where, ϕ is the angle between the inertial amplifier rods and the axis of the oscillators' motion. Assuming a small displacement, the small angle approximation means that this is effectively constant and u and v can be described in terms of $y_{1,2}$ as:

$$v = \frac{y_2 - y_1}{2} \quad \text{and} \quad u = \frac{y_2 - y_1}{2}\cot\phi \tag{6}$$

Using Eq. (2), the total kinetic energy of the system is:

$$T_{\text{total}} = \frac{1}{2}m\dot{y}_1^2 + \frac{1}{2}\gamma m\dot{y}_2^2 + \frac{1}{4}\mu m(\dot{y}_2 - \dot{y}_1)^2(1 + \cot^2\phi) \tag{7}$$

From this the partial derivatives of $\dot{y}_{1,2}$ can be obtained:

$$\frac{\partial T_{\text{total}}}{\partial \dot{y}_1} = \left(m + \frac{1}{2}\mu m(1 + \cot^2\phi)\right)\dot{y}_1 - \frac{1}{2}\mu m(1 + \cot^2\phi)\dot{y}_2 \tag{8}$$

$$\frac{\partial T_{\text{total}}}{\partial \dot{y}_2} = -\frac{1}{2}\mu m(1 + \cot^2\phi)\dot{y}_1 + \left(\gamma m + \frac{1}{2}\mu m(1 + \cot^2\phi)\right)\dot{y}_2 \tag{9}$$

These result in a mass matrix for the system of:

$$\mathbf{M} = m\begin{bmatrix} 1 + \frac{\mu}{2}(1 + \cot^2\phi) & -\frac{\mu}{2}(1 + \cot^2\phi) \\ -\frac{\mu}{2}(1 + \cot^2\phi) & \gamma + \frac{\mu}{2}(1 + \cot^2\phi) \end{bmatrix} \tag{10}$$

Using Eq. (4), the total potential energy of the system is:

$$U_{\text{total}} = \frac{1}{2}ky_1^2 + \frac{1}{2}\beta k(y_2 - y_1)^2 + \frac{1}{2}\alpha k y_2^2 + \frac{1}{2}\eta k\cot^2\phi(y_2 - y_1)^2 \tag{11}$$

From this the partial derivatives of $y_{1,2}$ can be obtained:

$$\frac{\partial U_{\text{total}}}{\partial y_1} = (k + \beta k + \eta k\cot^2\phi)y_1 - (\beta k + \eta k\cot^2\phi)y_2 \tag{12}$$

$$\frac{\partial U_{\text{total}}}{\partial y_2} = -(\beta k + \eta k\cot^2\phi)y_1 + (\alpha k + \beta k + \eta k\cot^2\phi)y_2 \tag{13}$$

These result in a stiffness matrix for the system of:

$$\mathbf{K} = k\begin{bmatrix} 1 + \beta + \eta\cot^2\phi & -\beta - \eta\cot^2\phi \\ -\beta - \eta\cot^2\phi & \alpha + \beta + \eta\cot^2\phi \end{bmatrix} \tag{14}$$

To simplify these equations and matrices, let:

$$\rho = \frac{1}{2}\mu(1 + \cot^2\phi) \quad \text{and} \quad \tau = \beta + \eta\cot^2\phi \tag{15}$$

This changes Eqs.(10) and (14) to:

$$\mathbf{M} = m\begin{bmatrix} 1 + \rho & -\rho \\ -\rho & \gamma + \rho \end{bmatrix} \tag{16}$$

$$\mathbf{K} = k\begin{bmatrix} 1 + \tau & -\tau \\ -\tau & \alpha + \tau \end{bmatrix} \tag{17}$$

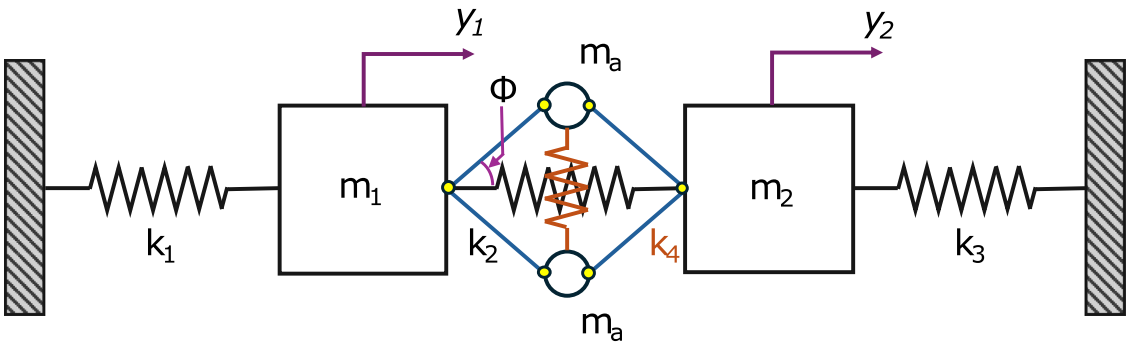

Fig. 1. A coupled double oscillator with both a connecting spring and stiffened inertial amplifier.

The equations of motion can be obtained using the system's Euler–Lagrange equations of the form:

$$\frac{\mathrm{d}}{\mathrm{d}t}\left(\frac{\partial L}{\partial \dot{y}}\right) - \frac{\partial L}{\partial y} = 0 \tag{18}$$

By combining Eqs.(8), (9), (12) and (13) in the form of Eq. (1) and applying Eq. (15), then the equations of motion for the system described in Fig. 1 are:

$$m(1+\rho)\ddot{y}_1 - \rho m\ddot{y}_2 = -k(1+\tau)y_1 + \tau k y_2 \tag{19a}$$

$$-\rho m\ddot{y}_1 + m(\gamma+\rho)\ddot{y}_2 = \tau k y_1 - k(\alpha+\tau)y_2 \tag{19b}$$

$$\mathbf{M}\begin{bmatrix}\ddot{y}_1\\ \ddot{y}_2\end{bmatrix} + \mathbf{K}\begin{bmatrix}y_1\\ y_2\end{bmatrix} = \begin{bmatrix}0\\ 0\end{bmatrix} \tag{20}$$

The stiffness matrix, Eq. (17), demonstrates the non-zero non-leading diagonal expected of the stiffness coupling inherent to a coupled double oscillator system where the two masses are connected solely by a spring. This is a common and well understood form due to the ubiquity of spring coupled systems. With the inclusion of an inertial amplifier, the mass matrix, Eq. (16), also gains a non-zero non-leading diagonal which indicates the presence of inertial coupling in the system. This, however, is a considerably more rare and little studied occurrence in comparison to spring coupling. If the connecting spring, τ, is removed and set to zero in the equations, the inertial coupling persists. This suggests the possibility of a purely inertial coupled system. While there is already precedence for inertial coupling, in existing literature this is mostly focused on soil or fluid mechanics, [20–25]. Within mechanical systems, inertial coupling is rarely if ever touched upon but, pure inertial coupling can be found in some circumstances such as coupled, or chaotic, pendulums [52,53].

As ρ and τ can be taken as being, respectively, the variables for any form of inertial and stiffness coupling then Eqs.(19) can be taken as the equations of motion for any undamped coupled double oscillator system, regardless of the exact composition of the coupling.

3. The analysis of the eigenvalues

The generalised eigenvalues are derived and the circumstances under which they will be distinct are determined.

3.1. Eigenvalue calculation

Take Eqs.(16) and (17) and apply them to the general equation of motion for a mass–spring system:

$$\mathbf{M}\ddot{y} + \mathbf{K}y = 0 \tag{21}$$

To find the eigenvalues of the system, let:

$$\det[\mathbf{K} - \lambda\mathbf{M}] = 0 \tag{22}$$

where λ are the eigenvalues. This determinant is:

$$(\gamma+\rho+\gamma\rho)m^2\lambda^2 - (\alpha+\gamma+\rho+\alpha\rho+\tau+\gamma\tau)km\lambda + (\alpha+\tau+\alpha\tau)k^2 = 0 \tag{23}$$

The determinant produces a quadratic equation in terms of λ which means that the eigenvalues of the system can be obtained using the formula:

$$\lambda_{1,2} = \frac{k}{m}\left(\frac{(\alpha+\gamma+\rho+\alpha\rho+\tau+\gamma\tau) \mp \sqrt{(\alpha+\gamma+\rho+\alpha\rho+\tau+\gamma\tau)^2 - 4(\gamma+\rho+\gamma\rho)(\alpha+\tau+\alpha\tau)}}{2(\gamma+\rho+\gamma\rho)}\right) \tag{24}$$

where the value of λ_1 is produced by the negative square root, while the value of λ_2 is produced by the positive square root. From these eigenvalues the respective natural frequencies can be obtained by taking the square root of λ. Eq. (24) applies to what can be considered a combined coupling system, with both inertial and stiffness coupling. In order to obtain the eigenvalues for a pure coupling system set ρ or τ to zero for pure inertial or pure stiffness coupling respectively.

3.2. Distinctiveness of the eigenvalues

It has already been demonstrated that the eigenvalues of a pure stiffness coupling double oscillator system will always be distinct. Stephen [51] used two methods to demonstrate this. One of their methods used matrices, taking advantage of the properties of Jacobi matrices to demonstrate that the eigenvalues of a pure stiffness, linear, series coupled dynamic system of up to infinite length are always distinct. Thus mode veering will inevitably always occur in such a system. This approach relies on the mass matrix of such a system being both diagonal and positive definite, which for inertial coupling is not the case. An inertial coupling mass matrix is, as with a stiffness coupling stiffness matrix, tridiagonal.

The other method Stephen used is specific to the coupled double oscillator system. They utilised the discriminant of the eigenvalue equation to demonstrate that the crossing of the eigenvalues was mathematically impossible in a pure stiffness coupling system and so mode veering would occur. The same approach can be taken for both combined coupling and pure inertial coupling coupled double oscillators. To do so, take the discriminant of Eq. (24):

$$k^2m^2((\alpha+\gamma+\rho+\alpha\rho+\tau+\gamma\tau)^2-4(\gamma+\rho+\gamma\rho)(\alpha+\tau+\alpha\tau)) \tag{25}$$

The loci of the eigenvalues, $\lambda_{1,2}$, will only cross if the discriminant is equal to zero. This can only occur if both ρ and τ are equal to each other, resulting in a discriminant of:

$$k^2m^2(\alpha-\gamma)^2(1+n)^2=0 \tag{26}$$

where $n=\rho=\tau$. Even in this case, the loci will only cross if $\alpha=\gamma$ as well. Except for this specific case, crossing of the loci will not occur. In the case of a system with pure inertial coupling, $\tau=0$, the discriminant can only be equal to zero if $\rho=0$ as well, and again only when $\alpha=\gamma$. In which case, as with a pure stiffness coupled double oscillator, the system will behave akin to uncoupled oscillators where:

$$k^2m^2(\alpha-\gamma)^2=(m_1k_3-m_2k_1)^2 \tag{27}$$

With an eigenvalue of:

$$\lambda_{uc}=\frac{k_1}{m_1}=\frac{k_3}{m_2} \tag{28}$$

Thus for a pure inertial coupled double oscillator system, the eigenvalues will always be distinct. As such, it can therefore be expected for mode veering to likewise always occur, along with its associated exchange of modal characteristics, for any pure inertially coupled double oscillator system and for any combined coupling system where the normalised coupling ratios are not equal.

4. Hyperbolic demonstration of mode veering

The approach used by Stephen, to demonstrate that mode veering will always occur in coupled double oscillators [51], builds upon the work done by Nair and Durvasula [54] as well as Chen and Ginsberg [55] to introduce new co-ordinate systems into the eigenvalue plots and re-frame the equations which describe them with respect to these new co-ordinates. By doing so, Stephen shows that the eigenvalue variance as a system parameter changes can be described as a hyperbola and as a hyperbola is always a hyperbolic curve for all potential variables, it can be demonstrated that eigenvalue veering will always occur in pure stiffness coupling double oscillator systems.

4.1. Pure inertial coupling veering for variable spring stiffness

By using the same approach it can be demonstrated that mode veering should likewise always occur in any coupled system with either inertial, stiffness or combined coupling. Take Eq. (23) for a system with pure inertial coupling, $\tau=0$, then the determinant, sometimes referred to as the frequency equation, of the system can be described as follows:

$$(\gamma+\rho+\gamma\rho)m^2\lambda^2-(\alpha+\gamma+\rho+\alpha\rho)km\lambda+\alpha k^2=0 \tag{29}$$

The eigenvalues of this system can thus be described as:

$$\lambda_{1,2}=\frac{k}{m}\frac{(\alpha+\gamma+\rho+\alpha\rho)\mp\sqrt{(\alpha+\gamma+\rho+\alpha\rho)^2-4\alpha(\gamma+\rho+\gamma\rho)}}{2(\gamma+\rho+\gamma\rho)} \tag{30}$$

As stated in Section 3.1, Eq. (30) is simply Eq. (24) where $\tau=0$. If the eigenvalues are plotted as α, the normalised stiffness of k_3, varies then the gradients of, the curvatures of and the gap between the eigenvalue loci are, respectively:

$$\frac{\partial\lambda_{1,2}}{\partial\alpha}=\frac{k}{m}\frac{1+\rho\mp\dfrac{2(1+\rho)(\alpha+\gamma+\rho+\alpha\rho)-4(\gamma+\rho+\gamma\rho)}{2\sqrt{(\alpha+\gamma+\rho+\alpha\rho)^2-4\alpha(\gamma+\rho+\gamma\rho)}}}{2(\gamma+\rho+\gamma\rho)} \tag{31}$$

$$\frac{\partial^2 \lambda_{1,2}}{\partial \alpha^2} = \mp \frac{k}{m} \frac{2\rho^2}{((\alpha+\gamma+\rho+\alpha\rho)^2 - 4\alpha(\gamma+\rho+\gamma\rho))^{\frac{3}{2}}} \tag{32}$$

$$\lambda_2 - \lambda_1 = \frac{k}{m} \frac{\sqrt{(\alpha+\gamma+\rho+\alpha\rho)^2 - 4\alpha(\gamma+\rho+\gamma\rho)}}{(\gamma+\rho+\gamma\rho)} \tag{33}$$

It can be found that the positions where the gradients are equal, the curvatures are maximum and the gap is minimum all occur for:

$$\alpha = \frac{\gamma+\rho+\gamma\rho-\rho^2}{(1+\rho)^2} \tag{34}$$

As this value of α is the same for all three of the above cases this location can be reasonably defined as being the point about which veering occurs. The midpoint of the minimum gap is at ordinate:

$$\lambda = \frac{k}{m}\frac{\alpha+\gamma+\rho+\alpha\rho}{2(\gamma+\rho+\gamma\rho)} = \frac{k}{m}\frac{1}{1+\rho}$$

It can be seen from Fig. 2 that this centre of veering also happens to be the intersection point of the two linear asymptotes. Thus the centre of veering can be defined as:

$$(\alpha_{\text{cov}}, \lambda_{\text{cov}}) = \left(\frac{\gamma+\rho+\gamma\rho-\rho^2}{(1+\rho)^2}, \frac{k}{m}\frac{1}{1+\rho}\right) \tag{35}$$

Now introduce a new co-ordinate system with its origin at this centre:

$$\kappa = \alpha - \alpha_{\text{cov}} \quad \text{and} \quad \Lambda = \lambda - \lambda_{\text{cov}} \tag{36}$$

When translated into this new co-ordinate system, Eq. (29) becomes:

$$(\gamma+\rho+\gamma\rho)m^2\Lambda^2 - \kappa k m(1+\rho)\Lambda - \frac{k^2\rho^2}{(1+\rho)^2} = 0 \tag{37}$$

The roots of this new polynomial, obtained using the quadratic formula, are:

$$\Lambda_{1,2} = \frac{k}{m} \frac{\kappa(1+\rho) \mp \sqrt{(-\kappa(1+\rho))^2 + 4(\gamma+\rho+\gamma\rho)\left(\frac{\rho^2}{(1+\rho)^2}\right)}}{2(\gamma+\rho+\gamma\rho)} \tag{38}$$

From these roots, the asymptotes of the eigenvalue loci curves can be obtained when $\kappa \to \infty$:

$$\Lambda_1 = 0 \quad \text{and} \quad \Lambda_2 = \frac{k}{m}\frac{\kappa(1+\rho)}{\gamma+\rho+\gamma\rho} \tag{39}$$

In terms of the original variables these, Fig. 2(a), are:

$$\lambda_1 = \frac{k}{m}\frac{1}{1+\rho} \quad \text{and} \quad \lambda_2 = \frac{k}{m}\frac{1}{1+\rho} + \frac{k}{m}\frac{1+\rho}{\gamma+\rho+\gamma\rho}\left(\alpha - \frac{\gamma+\rho+\gamma\rho-\rho^2}{(1+\rho)^2}\right) \tag{40}$$

Now, introduce an anti-clockwise rotation to the co-ordinates using:

$$\kappa = \kappa' \cos\theta - \Lambda' \sin\theta \quad \text{and} \quad \Lambda = \kappa' \sin\theta + \Lambda' \cos\theta \tag{41}$$

An anti-clockwise rotation is preferred to reveal vertical hyperbolae for ease of distinguishing between the first and second modes but a clockwise rotation will return the conjugate hyperbolae and so can also be used. As it is desired that the κ' axis to lie halfway between the asymptotes then:

$$\theta = \frac{\arctan\left(\frac{k}{m}\frac{1+\rho}{\gamma+\rho+\gamma\rho}\right)}{2} \tag{42}$$

Here, 2θ is the anti-clockwise, acute angle between the two asymptotes and can be used to describe the angle of deflection about the centre of veering. The larger this angle, the sharper the deflection and hence the stronger the veering phenomenon. The asymptotes, Eq. (39), can now be expressed in the new rotated co-ordinates:

$$\Lambda'_{1,2} = \mp\kappa' \frac{\sqrt{\left(\frac{k}{m}\frac{1+\rho}{\gamma+\rho+\gamma\rho}\right)^2 + 1} - 1}{\left(\frac{k}{m}\frac{1+\rho}{\gamma+\rho+\gamma\rho}\right)} \tag{43}$$

These asymptotes can be seen to be the asymptotes of a hyperbola of the form:

$$y = \mp\frac{b}{a}x \tag{44}$$

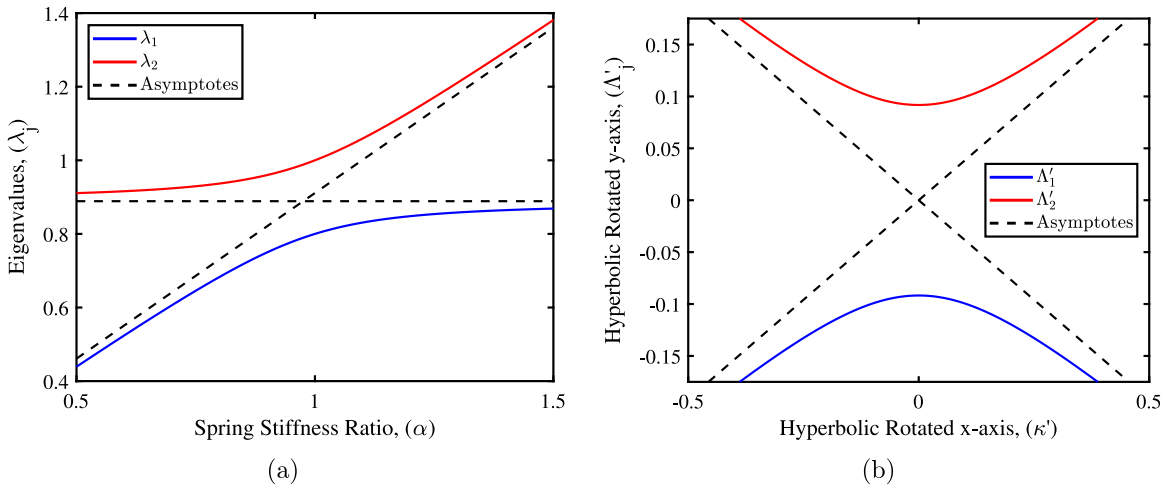

Fig. 2. The asymptotes of the eigenvalues (λ) with variable spring stiffness ratio (α), when plotted on rotated co-ordinates (κ', Λ') with their origin at the centre of veering ($\alpha_{cov}, \lambda_{cov}$), demonstrate the hyperbolic shape of eigenloci curves. (a) Stiffness Coupling (τ) = 0 and mass (m) = stiffness (k) = oscillator mass ratio (γ) = 1 with asymptotes. (b) Rotated co-ordinates demonstrating hyperbolic curvature.

where:

$$a = \left(\frac{k}{m}\frac{1+\rho}{\gamma+\rho+\gamma\rho}\right) \quad \text{and} \quad b = \sqrt{\left(\frac{k}{m}\frac{1+\rho}{\gamma+\rho+\gamma\rho}\right)^2 + 1} - 1 \tag{45}$$

Thus Eq. (37) can be expressed in the rotated co-ordinate system, Fig. 2(b), in the hyperbolic form:

$$\frac{\kappa'}{a^2} - \frac{\Lambda'}{b^2} = -1 \tag{46}$$

where the foci of the hyperbolas are found at:

$$\Lambda' = \mp\sqrt{a^2 + b^2} \tag{47}$$

The smaller the value of ρ the closer the two foci. It can also be seen that for all positive, finite values of ρ the change of eigenvalues with respect to α will always take the form of a hyperbola thus veering will always occur in a coupled double oscillator with pure inertial coupling.

4.2. Pure inertial coupling veering for variable mass

In a coupled double oscillator, as well as varying the spring stiffness ratio, α, the oscillator mass ratio, γ, can be varied as well. If for Eq. (30), the eigenvalues are plotted with respect to γ instead of α however, the resultant graph takes on a very different form, most notably the presence of non-linear asymptotes constraining the eigenvalue loci curves. To redefine the eigenvalue equation as a hyperbolic function it is necessary to describe the eigenvalue loci graph in such a way that the asymptotes are linear. The easiest way to do this is to change the ordinate λ to the inverse of the eigenvalues. By doing so, $\bar{\lambda} = \lambda^{-1}$ and Eq. (29) becomes:

$$\alpha k^2\bar{\lambda}^2 - (\alpha+\gamma+\rho+\alpha\rho)km\bar{\lambda} + (\gamma+\rho+\gamma\rho)m^2 = 0 \tag{48}$$

Thus the roots of this new polynomial, the inverse eigenvalues, are:

$$\bar{\lambda}_{1,2} = \frac{m}{k}\frac{(\alpha+\gamma+\rho+\alpha\rho) \mp \sqrt{(\alpha+\gamma+\rho+\alpha\rho)^2 - 4\alpha(\gamma+\rho+\gamma\rho)}}{2\alpha} \tag{49}$$

When the inverse eigenvalues are plotted as γ, oscillator mass ratio, varies then the gradients of, the curvatures of and the gap between the loci are, respectively:

$$\frac{\partial\bar{\lambda}_{1,2}}{\partial\gamma} = \frac{m}{k}\frac{1 \mp \dfrac{-4\alpha(1+\rho)+2(\alpha+\gamma+\rho+\alpha\rho)}{2\sqrt{(\alpha+\gamma+\rho+\alpha\rho)^2 - 4\alpha(\gamma+\rho+\gamma\rho)}}}{2\alpha} \tag{50}$$

$$\frac{\partial^2\bar{\lambda}_{1,2}}{\partial\gamma^2} = \mp\frac{m}{k}\frac{2\rho^2}{((\alpha+\gamma+\rho+\alpha\rho)^2 - 4\alpha(\gamma+\rho+\gamma\rho))^{\frac{3}{2}}} \tag{51}$$

$$\bar{\lambda}_2 - \bar{\lambda}_1 = \frac{m}{k}\frac{\sqrt{(\alpha+\gamma+\rho+\alpha\rho)^2 - 4\alpha(\gamma+\rho+\gamma\rho)}}{\alpha} \tag{52}$$

It can be found that the positions where the gradients are equal, the curvatures are maximum and the gap is minimum all occur for:

$$\gamma = \alpha - \rho + \alpha\rho \tag{53}$$

As this value of γ is the same for all three of the above cases, this location can be reasonably defined as being the point about which veering occurs. The midpoint of the minimum gap is at ordinate:

$$\bar{\lambda} = \frac{m}{k}\frac{\alpha+\gamma+\rho+\alpha\rho}{2\alpha} = \frac{m}{k}(1+\rho) \tag{54}$$

Thus the centre of veering can be defined as:

$$(\gamma_{\text{cov}}, \bar{\lambda}_{\text{cov}}) = \left(\alpha - \rho + \alpha\rho, \frac{m}{k}(1+\rho)\right) \tag{55}$$

Now introduce a new co-ordinate system with its origin at this centre:

$$\zeta = \gamma - \gamma_{\text{cov}} \quad \text{and} \quad \bar{\Lambda} = \bar{\lambda} - \bar{\lambda}_{\text{cov}} \tag{56}$$

When translated into this new co-ordinate system, Eq. (48) becomes:

$$\alpha k^2 \bar{\Lambda}^2 - \zeta k m \bar{\Lambda} - m^2\rho^2 = 0 \tag{57}$$

The roots of this new polynomial, obtained using the quadratic formula, are:

$$\bar{\Lambda}_{1,2} = \frac{m}{k}\frac{\zeta \mp \sqrt{(-\zeta)^2 + 4\alpha\rho^2}}{2\alpha} \tag{58}$$

From these roots, the asymptotes of the inverse eigenvalue loci curves can be obtained when $\zeta \to \infty$:

$$\bar{\Lambda}_1 = 0 \quad \text{and} \quad \bar{\Lambda}_2 = \frac{m}{k}\frac{\zeta}{\alpha} \tag{59}$$

In terms of the inverse eigenvalues, Fig. 3(a), these are:

$$\bar{\lambda}_1 = \frac{m}{k}(1+\rho) \quad \text{and} \quad \bar{\lambda}_2 = \frac{m}{k}\left(\frac{\gamma - \alpha + \rho - \alpha\rho}{\alpha} + 1 + \rho\right) \tag{60}$$

Now, introduce an anti-clockwise co-ordinate rotation using:

$$\zeta = \zeta' \cos\theta - \bar{\Lambda}' \sin\theta \quad \text{and} \quad \bar{\Lambda} = \zeta' \sin\theta + \bar{\Lambda}' \cos\theta \tag{61}$$

As it is desirable that the ζ' axis to lie halfway between the asymptotes then:

$$\theta = \frac{\arctan\left(\frac{m}{k\alpha}\right)}{2} \tag{62}$$

Now express the asymptotes, Eq. (59), in the new, rotated co-ordinates:

$$\bar{\Lambda}'_{1,2} = \mp\zeta' \frac{\sqrt{\left(\frac{m}{k\alpha}\right)^2 + 1} - 1}{\frac{m}{k\alpha}} \tag{63}$$

These can be seen to be the asymptotes of a hyperbola of the form Eq. (44), where:

$$a = \frac{m}{k\alpha} \quad \text{and} \quad b = \sqrt{\left(\frac{m}{k\alpha}\right)^2 + 1} - 1 \tag{64}$$

Thus Eq. (57) can be expressed in the rotated co-ordinate system, Fig. 3(b), in the hyperbolic form:

$$\frac{\zeta'}{a^2} - \frac{\bar{\Lambda}'}{b^2} = -1 \tag{65}$$

where the foci of the hyperbolas are found using Eq. (47).

4.3. Combined coupling veering

The same hyperbolic method can be applied to a combined coupling case.

4.3.1. Variable spring stiffness

For Eq. (23) when the eigenvalues from Eq. (24) are plotted against α then the gradients of, the curvatures of and the gap between the loci are, respectively:

$$\frac{\partial\lambda_{1,2}}{\partial\alpha} = \left(\frac{k}{m}\right)\frac{1}{2(\gamma+\rho+\gamma\rho)}\left(1 + \rho \mp \frac{2(1+\rho)(\alpha+\gamma+\rho+\alpha\rho+\tau+\gamma\tau) - 4(\gamma+\rho+\gamma\rho)(1+\tau)}{\sqrt{(\alpha+\gamma+\rho+\alpha\rho+\tau+\gamma\tau)^2 - 4(\gamma+\rho+\gamma\rho)(\alpha+\tau+\alpha\tau)}}\right) \tag{66}$$

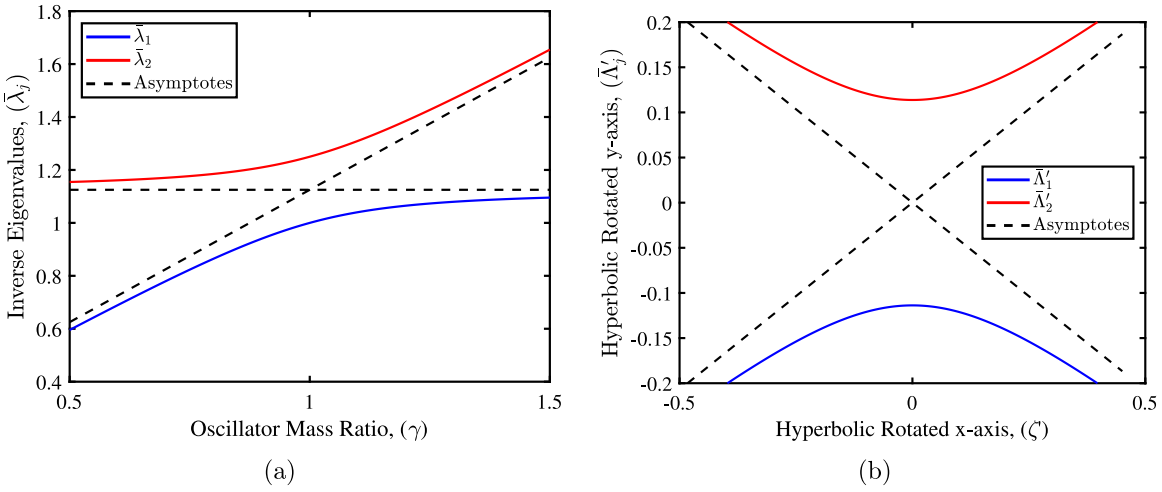

Fig. 3. The asymptotes of the inverse eigenvalues $(\bar{\lambda})$ with variable oscillator mass ratio (γ), when plotted on rotated co-ordinates $(\zeta', \bar{\Lambda}')$ with their origin at the centre of veering $(\gamma_{\text{cov}}, \bar{\lambda}_{\text{cov}})$, demonstrate the hyperbolic shape of inverse eigenloci curves. (a) Inverse eigenvalues $(\bar{\lambda})$ for stiffness coupling $(\tau) = 0$ and mass (m) = stiffness (k) = spring stiffness ratio $(\alpha) = 1$ with asymptotes. (b) Rotated co-ordinates demonstrating hyperbolic curvature.

$$\frac{\partial^2 \lambda_{1,2}}{\partial \alpha^2} = \mp \frac{k}{m} \frac{2(\rho-\tau)^2}{((\alpha+\gamma+\rho+\alpha\rho+\tau+\gamma\tau)^2 - 4(\gamma+\rho+\gamma\rho)(\alpha+\tau+\alpha\tau))^{\frac{3}{2}}} \tag{67}$$

$$\lambda_2 - \lambda_1 = \frac{k}{m} \frac{\sqrt{(\alpha+\gamma+\rho+\alpha\rho+\tau+\gamma\tau)^2 - 4(\gamma+\rho+\gamma\rho)(\alpha+\tau+\alpha\tau)}}{(\gamma+\rho+\gamma\rho)} \tag{68}$$

It can be found that the positions where the gradients are equal, the curvatures are maximum and the gap is minimum all occur for:

$$\alpha = \frac{\gamma+\rho+\gamma\rho-\rho^2-\tau+\gamma\tau+\rho\tau+\gamma\rho\tau}{(1+\rho)^2} \tag{69}$$

As this value of α is the same for all three of the above cases, this location can reasonably defined as being the point about which veering occurs. The midpoint of the minimum gap is at ordinate:

$$\lambda = \frac{k}{m}\frac{1+\tau}{1+\rho} \tag{70}$$

Thus the centre of veering can be defined as:

$$(\alpha_{\text{cov}}, \lambda_{\text{cov}}) = \left(\frac{\gamma+\rho+\gamma\rho-\rho^2-\tau+\gamma\tau+\rho\tau+\gamma\rho\tau}{(1+\rho)^2}, \frac{k}{m}\frac{1+\tau}{1+\rho} \right) \tag{71}$$

Now introduce a new co-ordinate system with its origin at this centre, Eq. (36). When translated into this new co-ordinate system, Eq. (23) becomes:

$$(\gamma+\rho+\gamma\rho)m^2\Lambda^2 - (1+\rho)km\kappa\Lambda - \frac{k^2(\rho-\tau)^2}{(1+\rho)^2} = 0 \tag{72}$$

The roots of this new polynomial can be obtained using the quadratic formula and from these, the asymptotes of the eigenvalue loci curves can be obtained when $\kappa \to \infty$:

$$\Lambda_1 = 0 \quad \text{and} \quad \Lambda_2 = \frac{k}{m}\frac{\kappa(1+\rho)}{\gamma+\rho+\gamma\rho} \tag{73}$$

In terms of the original variables these are:

$$\lambda_1 = \frac{k}{m}\frac{1+\tau}{1+\rho} \tag{74a}$$

$$\lambda_2 = \frac{k}{m}\left(\frac{1+\tau}{1+\rho} + \frac{1+\rho}{\gamma+\rho+\gamma\rho}\left(\alpha - \frac{\gamma+\rho+\gamma\rho-\rho^2-\tau+\gamma\tau+\rho\tau+\gamma\rho\tau}{(1+\rho)^2} \right) \right) \tag{74b}$$

Now, introduce an anti-clockwise rotation to the co-ordinates using Eq. (41). As it is desirable for the κ' axis to lie halfway between the asymptotes. Note how Eqs.(39) and (73) are the same. Thus θ is defined by Eq. (42). From this it is known that the asymptotes in the new, rotated co-ordinates are defined by Eq. (43) and that Eq. (72) can be expressed in the rotated co-ordinate system in the hyperbolic form defined by Eqs.(45) and (46).

From this it is evident that as long $\rho \neq \tau$ then for any positive, finite values of ρ and τ, the change of the eigenvalues with respect to α will always take the form of a hyperbola. Thus veering will always occur in a coupled double oscillator with any combination of inertial and stiffness coupling except for the specific case of $\rho = \tau$.

4.3.2. Variable mass

The same approach can also be followed for variable mass with combined coupling by utilising the inverse eigenvalues which can be obtained using $\bar{\lambda} = \lambda^{-1}$, thus Eq. (23) becomes:

$$(\alpha + \tau + \alpha\tau)k^2\bar{\lambda}^2 - (\alpha + \gamma + \rho + \alpha\rho + \tau + \gamma\tau)km\bar{\lambda} + (\gamma + \rho + \gamma\rho)m^2 = 0 \tag{75}$$

When the inverse eigenvalues, obtained from the roots of the polynomial Eq. (75), are plotted against γ then the gradients of, the curvatures of and the gap between the loci are, respectively:

$$\frac{\partial\bar{\lambda}_{1,2}}{\partial\gamma} = \frac{m}{k}\frac{1+\tau \pm \dfrac{(\rho-\tau)(\tau-1)+\alpha(1+\rho)(1+\tau)-\gamma(1+\tau)^2}{\sqrt{(\alpha+\gamma+\rho+\alpha\rho+\tau+\gamma\tau)^2-4(\gamma+\rho+\gamma\rho)(\alpha+\tau+\alpha\tau)}}}{2(\alpha+\tau+\alpha\tau)} \tag{76}$$

$$\frac{\partial^2\bar{\lambda}_{1,2}}{\partial\gamma^2} = \mp\frac{m}{k}\frac{2(\rho-\tau)^2}{((\alpha+\gamma+\rho+\alpha\rho+\tau+\gamma\tau)^2-4(\gamma+\rho+\gamma\rho)(\alpha+\tau+\alpha\tau))^{\frac{3}{2}}} \tag{77}$$

$$\bar{\lambda}_2 - \bar{\lambda}_1 = \frac{m}{k}\frac{\sqrt{(\alpha+\gamma+\rho+\alpha\rho+\tau+\gamma\tau)^2-4(\gamma+\rho+\gamma\rho)(\alpha+\tau+\alpha\tau)}}{(\alpha+\tau+\alpha\tau)} \tag{78}$$

It can be found that the positions where the gradients are equal, the curvatures are maximum and the gap is minimum all occur for:

$$\gamma = \frac{\alpha+\tau+\alpha\tau-\tau^2-\rho+\alpha\rho+\rho\tau+\alpha\rho\tau}{(1+\tau)^2} \tag{79}$$

As this value of γ is the same for all three of the above cases, this location can reasonably defined as being the point about which veering occurs. The midpoint of the minimum gap is at ordinate:

$$\bar{\lambda} = \frac{m}{k}\frac{1+\rho}{1+\tau} \tag{80}$$

So the centre of veering can be defined as:

$$(\gamma_{\text{cov}}, \bar{\lambda}_{\text{cov}}) = \left(\frac{\alpha+\tau+\alpha\tau-\tau^2-\rho+\alpha\rho+\rho\tau+\alpha\rho\tau}{(1+\tau)^2}, \frac{m}{k}\frac{1+\rho}{1+\tau}\right) \tag{81}$$

Now introduce a new co-ordinate system with its origin at this centre, Eq. (56). When translated into this new co-ordinate system, Eq. (75) becomes:

$$(\alpha+\tau+\alpha\tau)k^2\Lambda^2 - (1+\tau)km\zeta\Lambda - m^2\frac{(\rho-\tau)^2}{(1+\tau)^2} = 0 \tag{82}$$

The asymptotes of the inverse eigenvalue loci curves can be obtained from the roots of this new polynomial when $\zeta \to \infty$:

$$\Lambda_1 = 0 \quad \text{and} \quad \Lambda_2 = \frac{m}{k}\frac{\zeta(1+\tau)}{\alpha+\tau+\alpha\tau} \tag{83}$$

In terms of the original variables these are:

$$\bar{\lambda}_1 = \frac{m}{k}\frac{1+\rho}{1+\tau} \tag{84a}$$

$$\bar{\lambda}_2 = \frac{m}{k}\left(\frac{1+\rho}{1+\tau} + \frac{1+\tau}{\alpha+\tau+\alpha\tau}\left(\gamma - \frac{\alpha+\tau+\alpha\tau-\tau^2-\rho+\alpha\rho+\rho\tau+\alpha\rho\tau}{(1+\tau)^2}\right)\right) \tag{84b}$$

Now, introduce an anti-clockwise rotation to the co-ordinates using Eq. (61). As it is desirable for the ζ' axis to lie halfway between the asymptotes then:

$$\theta = \frac{\arctan\left(\dfrac{m}{k}\dfrac{1+\tau}{\alpha+\tau+\alpha\tau}\right)}{2} \tag{85}$$

Now express the asymptotes, Eq. (83), in the new rotated co-ordinates:

$$\Lambda'_{1,2} = \mp\zeta'\frac{\sqrt{\left(\dfrac{m}{k}\dfrac{1+\tau}{\alpha+\tau+\alpha\tau}\right)^2+1}-1}{\dfrac{m}{k}\dfrac{1+\tau}{\alpha+\tau+\alpha\tau}} \tag{86}$$

These can be seen to be the asymptotes of a hyperbola of the form Eq. (44), where:

$$a = \frac{m}{k}\frac{1+\tau}{\alpha+\tau+\alpha\tau} \quad \text{and} \quad b = \sqrt{\left(\frac{m}{k}\frac{1+\tau}{\alpha+\tau+\alpha\tau}\right)^2+1}-1 \tag{87}$$

Table 1
The centre of veering and hyperbolic asymptotes for pure coupling systems.

Coupling type	Pure stiffness	Pure inertial
Centre of veering $(\alpha_{\text{cov}}, \lambda_{\text{cov}})$	$\left(\gamma - \tau + \gamma\tau, \frac{k}{m}(1+\tau)\right)$	$\left(\frac{\gamma+\rho+\gamma\rho-\rho^2}{(1+\rho)^2}, \frac{k}{m}\frac{1}{1+\rho}\right)$
Centre of veering $(\gamma_{\text{cov}}, \bar{\lambda}_{\text{cov}})$	$\left(\frac{\alpha+\tau+\alpha\tau-\tau^2}{(1+\tau)^2}, \frac{m}{k}\frac{1}{1+\tau}\right)$	$\left(\alpha - \rho + \alpha\rho, \frac{m}{k}(1+\rho)\right)$
Hyperbolic asymptotes[a], Variable α	$a = \frac{k}{m\gamma}$	$a = \frac{k}{m}\frac{1+\rho}{\gamma+\rho+\gamma\rho}$
Hyperbolic asymptotes[a], Variable γ	$a = \frac{m}{k}\frac{1+\tau}{\alpha+\tau+\alpha\tau}$	$a = \frac{m}{k\alpha}$

[a] From Eq. (44) where $b = \sqrt{a^2+1} - 1$.

Table 2
The centre of veering and hyperbolic asymptotes for combined coupling systems.

Variable	Centre of veering	Hyperbolic asymptotes[a]
α	$\left(\frac{\gamma+\rho+\gamma\rho-\rho^2-\tau+\gamma\tau+\rho\tau+\gamma\rho\tau}{(1+\rho)^2}, \frac{k}{m}\frac{1+\tau}{1+\rho}\right)$	$a = \frac{k}{m}\frac{1+\rho}{\gamma+\rho+\gamma\rho}$
γ	$\left(\frac{\alpha+\tau+\alpha\tau-\tau^2-\rho+\alpha\rho+\rho\tau+\alpha\rho\tau}{(1+\tau)^2}, \frac{m}{k}\frac{1+\rho}{1+\tau}\right)$	$a = \frac{m}{k}\frac{1+\tau}{\alpha+\tau+\alpha\tau}$

[a] From Eq. (44) where $b = \sqrt{a^2+1} - 1$.

Thus Eq. (82) can be expressed in the rotated co-ordinate system in the hyperbolic form of Eq. (65).

From this it is also evident that as long as $\rho \neq \tau$ then for any positive, finite values of ρ and τ, the change of the inverse eigenvalues with respect to γ will always take the form of a hyperbola. Thus veering will always occur in a coupled double oscillator with any combination of inertial and stiffness coupling except for the specific case of $\rho = \tau$.

5. System symmetry

As has already been noted, mode veering is related to the symmetry of a system and as such, if such potential symmetries are identified then the mode veering phenomenon can be described for any potential set of system parameters.

5.1. Coupling inverse symmetry

If the centre of veering and the hyperbolic asymptotes of the two pure coupling cases, pure stiffness and pure inertial coupling, are compared, Table 1, it can be observed that there is an inverse symmetry between the two coupling systems. When $\rho = 0$, the centre of veering and the hyperbolic asymptotes for variable α take the same general form as those for $\tau = 0$ for variable γ. Additionally, when $\rho = 0$, the centre of veering and the hyperbolic asymptotes for variable γ take the same general form as those for $\tau = 0$ and variable α. It can also be seen that to switch from one system to the other swap m with k, α with γ, ρ with τ and λ with $\bar{\lambda}$.

When looking at the centre of veering and the hyperbolic asymptotes for a combined coupling system, Table 2, this inverse symmetry continues. The general forms of both the centre of veering and the hyperbolic asymptotes, are the same. The difference between them is that m and k, α and γ, ρ and τ and λ and $\bar{\lambda}$ are swapped. Furthermore, the hyperbolic asymptotes for the combined coupling case are identical to the pure coupling cases, with the asymptotes for variable α being the same as for the pure inertial coupling case and the asymptotes for variable γ being the same as the pure stiffness coupling case. It is evident that the centre of veering and the hyperbolic asymptotes of the two pure coupling cases are simpler forms of the combined coupling case. It is also observable that, in the hyperbolic domain, for variable α, neither α nor τ have any influence over the asymptotes and hence the shape of the hyperbola. While for variable γ, neither γ nor ρ have any influence over the asymptotes or the shape of the hyperbola. For cases where $\rho = \tau = n$, the centre of veering reduces down to:

$$(\alpha_{\text{cov}}, \lambda_{\text{cov}}) = \left(\gamma, \frac{k}{m}\right) \quad \text{and} \quad (\gamma_{\text{cov}}, \bar{\lambda}_{\text{cov}}) = \left(\alpha, \frac{m}{k}\right) \tag{88}$$

When the roots of the polynomials given in Eqs.(72) and (82) are taken, for cases where $\rho = \tau = n$, the following equations are obtained:

$$\Lambda_{1,2} = \frac{k}{m}\frac{(1+n)\kappa \mp \sqrt{(1+n)^2\kappa^2}}{2(\gamma+n+\gamma n)} \tag{89}$$

$$\bar{\Lambda}_{1,2} = \frac{m}{k}\frac{(1+n)\zeta \mp \sqrt{(1+n)^2\zeta^2}}{2(\alpha+n+\alpha n)} \tag{90}$$

If the asymptotes for $\kappa \to \infty$ and $\zeta \to \infty$ are compared to the results of the two equations, it can be seen that they are same. In other words, the eigenvalues in the new co-ordinate systems are the same as the asymptotes deduced from the quadratic formulae. This can be checked by obtaining the curvatures of Eqs.(23) and (75) for the case where $\rho = \tau$ for variable α and γ, the result is

zero. Thus it can be conclude that no curvature occurs for this case and hence there is no hyperbola and thus no mode veering. Hence the centre of veering instead becomes the point at which the eigenvalue loci cross. Considering these reductions a combined coupling system with $\rho = \tau$ could be conceived as being symmetric and as slight asymmetries in a dynamic system give rise to mode veering [54,56], this is why significant mode veering can occur for any value of ρ and τ when they are close in size, even when both are very large. Unlike in pure coupling systems where one must be zero and the other must be small to produce significant mode veering.

5.2. System point of symmetry

The points given by Eq. (88) can be described as being the system's point of symmetry. This being the point at which the coupled double oscillator system has the necessary symmetry to possess non-distinct eigenvalues. If the pure coupling cases are considered to be simply specific forms of the more general coupled coupling case then some distinctive behaviour of the eigenvalue curves relating to this symmetry point are predictable if this consideration holds true. To do so, take the variable stiffness case, where α changes as outlined in Section 4.3.1. Let $\alpha = \alpha_{\text{cov}}$ as given by Eq. (88). Thus, Eq. (24) will simplify to:

$$\lambda = \frac{k}{m} \frac{(\rho + \tau + \gamma(2 + \rho + \tau)) \mp \sqrt{(1+\gamma)^2(\rho - \tau)^2}}{2(\gamma + \rho + \gamma\rho)} \tag{91}$$

Assuming that $\gamma|\rho|\tau > 0$, which for any real system they should be, then the eigenvalues at the point of symmetry are:

$$\lambda = \frac{k}{m} \quad \text{and} \quad \lambda = \frac{k}{m} \frac{\gamma + \tau + \gamma\tau}{\gamma + \rho + \gamma\rho} \tag{92}$$

where:

$$\frac{k}{m} = \begin{cases} \lambda_1, & \text{if } \tau > \rho \\ \lambda_2, & \text{if } \rho > \tau \\ \lambda_{1,2}, & \text{if } \rho = \tau \end{cases}$$

This means that when $\rho > \tau$ changes to either ρ or τ should result in the λ_1 curves shifting up and down while all the λ_2 curves intersect the symmetry point. While when $\tau > \rho$ changes to either ρ or τ should result in the λ_2 curves shifting up and down while all the λ_1 curves intersect the symmetry point. As this holds true for all values of ρ and τ then it should also hold true for the pure coupling cases as well.

If the proposal that it is the symmetry, or lack thereof, of a system that permits or prohibits non-distinct eigenvalues [54,56] is considered, then Eqs.(88) and (92) show that for a double coupled oscillator there are two pairs of variables that represent the symmetry of the system. The first pair is α and γ and the second is ρ and τ. Thus non-distinct eigenvalues can be considered as being the eigenvalues for a complete symmetry, these are given by λ_{cov} in Eq. (88), which can also be referred to as the symmetric eigenvalue. This gives rise to three possible outcomes. First, when neither of the variables in either of the two pairs are equal then none of the eigenvalue loci can be equal to the symmetric eigenvalue. Second, when one of the pairs, usually α and γ, are equal, then one of the eigenvalue loci can be equal to the symmetric eigenvalue. Third, when both pairs have equal variables then the system has sufficient symmetry to support both eigenvalue loci being equal to the symmetric eigenvalue. Considering the above, it is clear that neither eigenvalue curve can cross over from one side of the point of symmetry to the other. When α or γ are varied, one of the eigenvalue curves will always intersect this point and as ρ and τ get closer and closer, the other curve will approach and eventually also intersect when the values are equal and complete symmetry is achieved.

6. Mode veering

Through the following graphs and discussions of them the influence of inertial coupling on mode veering and how the system symmetries affect the dynamic behaviour of the system. This is divided up into four sections, an overview of the pure stiffness case, a comparison with the pure inertial case, an analysis of the combined coupling case and a discussion on the behaviour around the point of symmetry.

6.1. Pure stiffness coupling

With pure stiffness coupling there is only one variable which can influence the nature of the oscillator coupling, the coupling stiffness, τ, Fig. 4(a) and (b). Changes in τ adjust the minimum gap, the gradient and the curvature of the eigenvalue loci, as $\tau \to 0$ the minimum gap decreases and the maximum curvature increases.

In addition, as predicted in Section 5.2, the λ_2 curves vary position with τ while all of the λ_1 curves intersect the point of symmetry, in this case at $\lambda = 1$ and either $\alpha = 1$, for Fig. 4(a), or $\gamma = 1$ for Fig. 4(b).

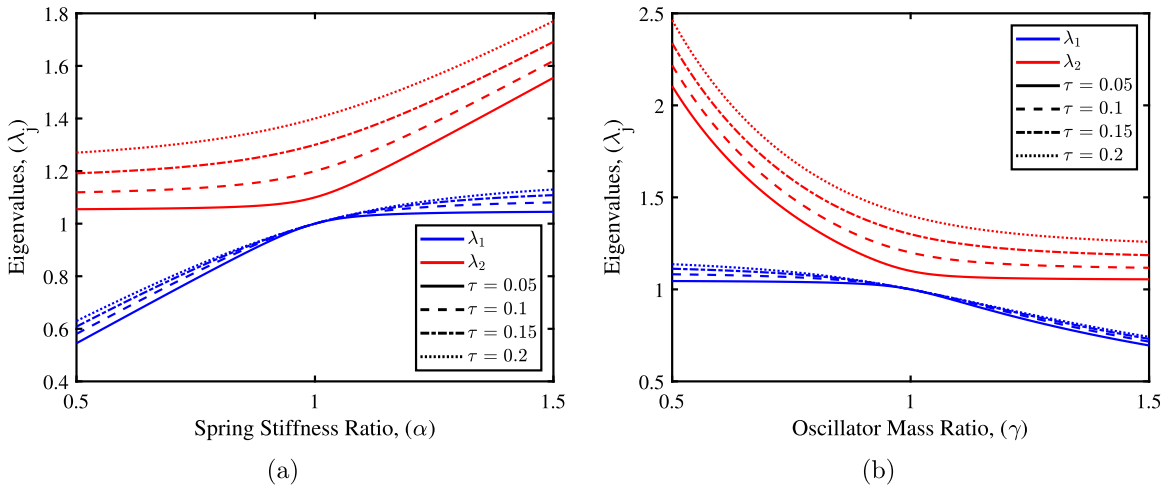

Fig. 4. Mode veering for pure stiffness coupling with several different values of stiffness coupling (τ) and either variable spring stiffness ratio (α) or variable oscillator mass ratio (γ). (a) Inertial Coupling (ρ) = 0 and mass m = stiffness (k) = oscillator mass ratio (γ) = 1 (b) Inertial Coupling (ρ) = 0 and mass m = stiffness (k) = spring stiffness ratio (α) = 1.

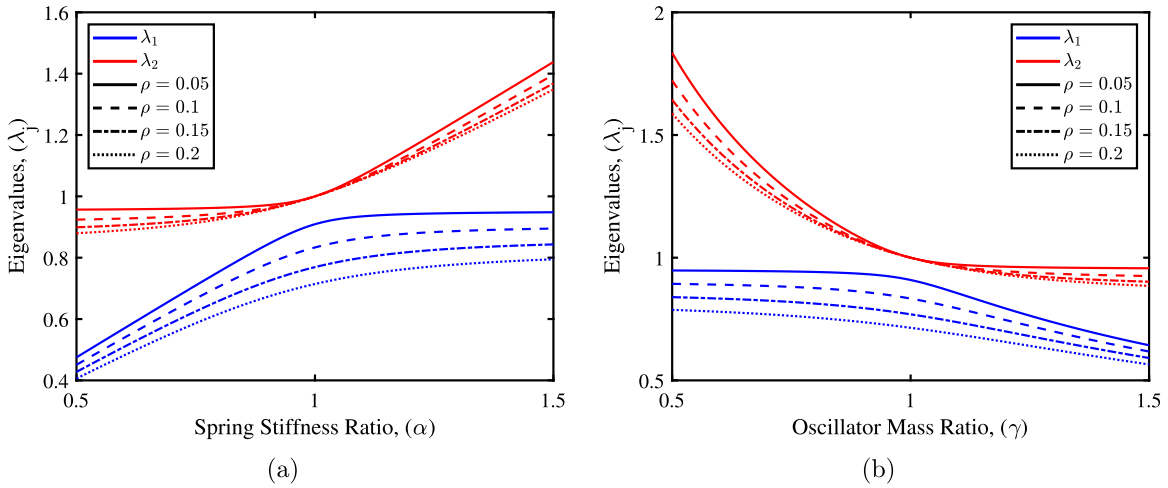

Fig. 5. Mode veering for pure inertial coupling with several different values of inertial coupling (ρ) and either variable spring stiffness ratio (α) or variable oscillator mass ratio (γ). (a) Stiffness Coupling (τ) = 0 and mass m = stiffness (k) = oscillator mass ratio (γ) = 1 (b) Stiffness Coupling (τ) = 0 and mass m = stiffness (k) = spring stiffness ratio (α) = 1.

6.2. Pure inertial coupling

When the pure stiffness coupling is replaced by pure inertial coupling, the sole variable influencing the nature of the oscillator coupling is changed to the inertial coupling, ρ. It can also be observed that mode veering still occurs with the general shapes of the eigenvalue loci being very similar to those of the pure stiffness coupling cases, Fig. 5(a) and (b). As with τ for the pure stiffness case, in this pure inertial case, changes in ρ adjusts the minimum gap, the gradient and the curvature of the eigenvalue loci. As $\rho \to 0$ the minimum gap decreases and the maximum curvature increases.

Once again, as predicted in Section 5.2, this time the λ_1 curves vary position with ρ while all of the λ_2 curves intersect the point of symmetry, in this case at $\lambda = 1$ and either $\alpha = 1$, for Fig. 5(a) or $\gamma = 1$ for Fig. 5(b).

6.3. Combined coupling

When both stiffness and inertial coupling are present in the same system, the influence of ρ and τ are expanded to affect both eigenvalue loci, λ_1 and λ_2, depending upon their relative sizes, Figs. 6(a) to 7(b). As predicted in Section 5.2, when $\rho > \tau$, it is the λ_1 curve that shifts as either ρ or τ are changed. But when $\rho < \tau$ then it is the λ_2 curve that shifts up and down instead. It is evident

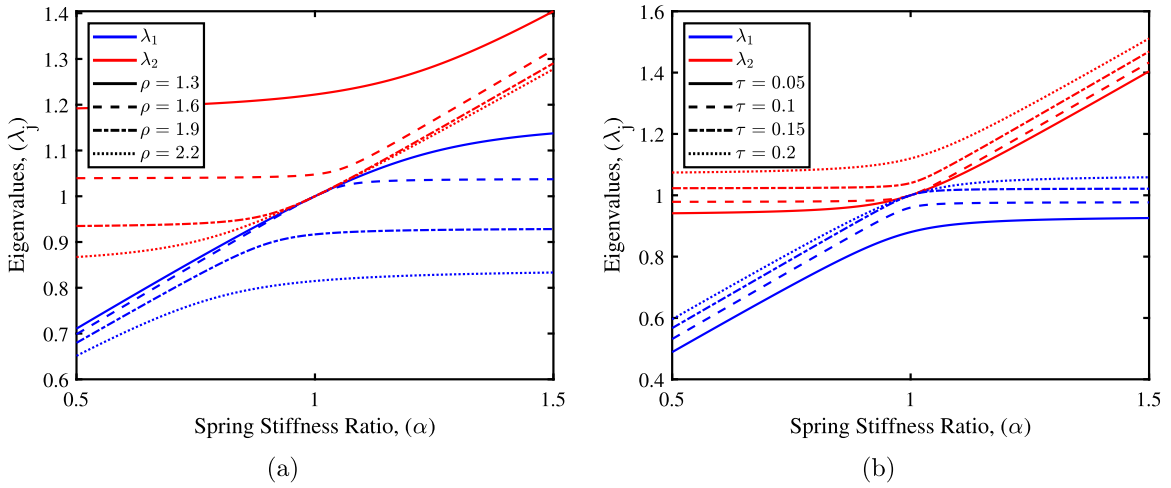

Fig. 6. Mode veering for combined coupling with variable spring stiffness ratio (α) and several different values of either inertial coupling (ρ) or stiffness coupling (τ). (a) Stiffness Coupling (τ) = 1.7 and mass m = stiffness (k) = oscillator mass ratio (γ) = 1 (b) Inertial Coupling (ρ) = 0.125 and mass m = stiffness (k) = oscillator mass ratio (γ) = 1.

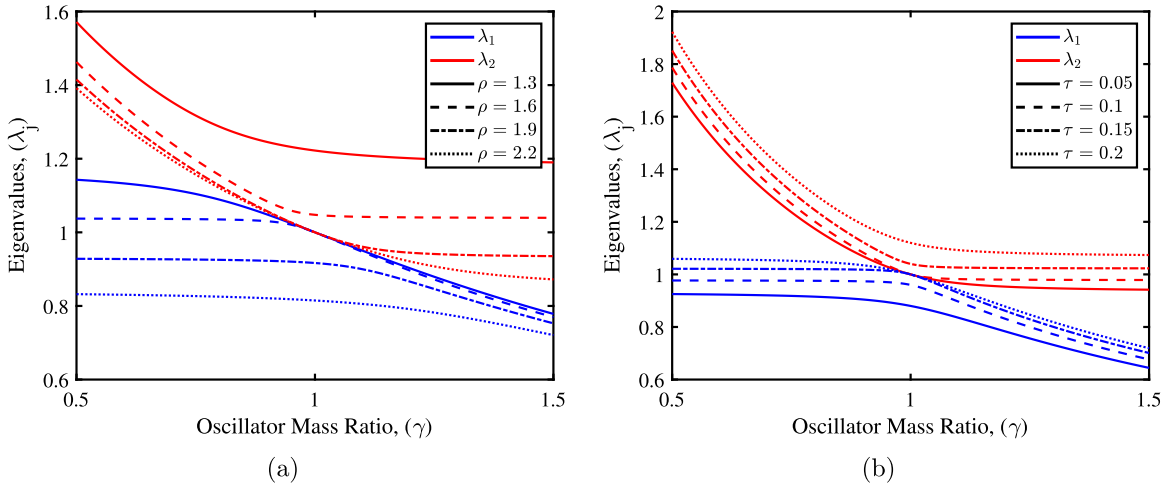

Fig. 7. Mode veering for combined coupling with variable oscillator mass ratio (γ) and several different values of either inertial coupling (ρ) or stiffness coupling (τ). (a) Stiffness Coupling (τ) = 1.7 and mass m = stiffness (k) = spring stiffness ratio (α) = 1 (b) Inertial Coupling (ρ) = 0.125 and mass m = stiffness (k) = spring stiffness ratio (α) = 1.

that for both the combined coupling graphs and the pure coupling graphs that this behaviour holds true regardless of whether or not either ρ or τ are equal to zero.

These graphs can also be used to confirm the supposition that mode veering would occur for any case where $\rho \to \tau$, regardless of the size of ρ or τ, Figs. 6(a) and 7(a). Therefore, when inertial and stiffness coupling are combined, significant mode veering could be induced even for very high stiffness coupling cases, should the magnitudes of the normalised stiffness coupling and the normalised inertial coupling be similar.

6.4. Point of symmetry

If the point of symmetry is highlighted on the mode veering graphs it is even more easily observed that one of the eigenvalue loci curves will always pass through this point and that neither set of curves can cross from one side of the point to the other, Fig. 8(a). Here, Fig. 9(a) and (b) demonstrate that the pure coupling cases follow this behaviour, further demonstrating that they are merely specific cases of a general combined coupling behaviour where ρ or τ are equal to zero. In Section 5.2, it was also proposed that as long as either $\alpha = \gamma$ or $\rho = \tau$, one of the eigenvalue curves would intersect the point of symmetry, Fig. 8(b) demonstrates this is the case by varying ρ instead of α and having several eigenvalue loci curves for different constants of α instead of ρ or τ.

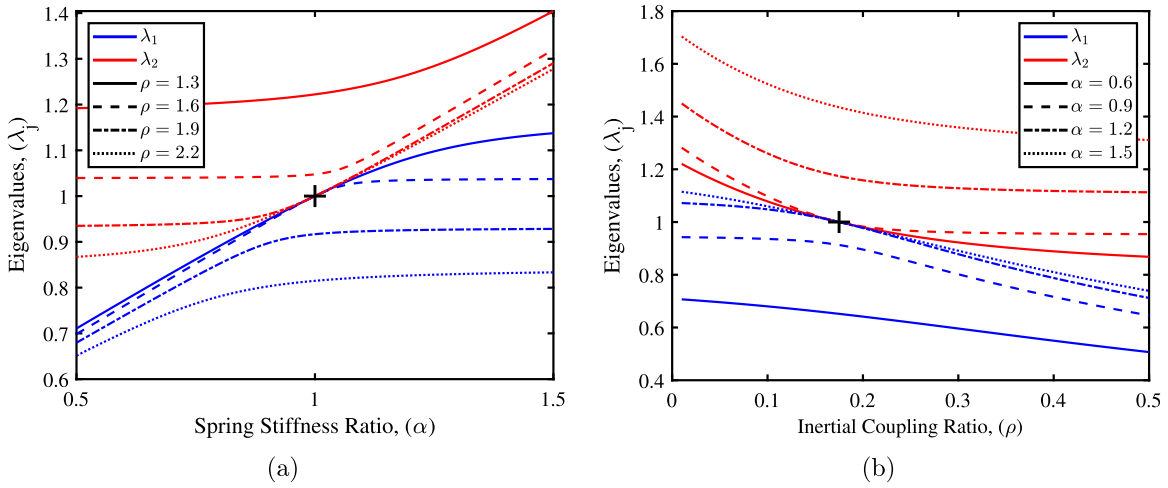

Fig. 8. Mode veering for combined coupling with the system's point of symmetry highlighted by the black cross. When α, γ, ρ or τ are varied, one eigenvalue loci curve always intersects the point of symmetry. (a) Stiffness coupling (τ) = 1.7 and mass (m) = stiffness (k) = oscillator mass ratio (γ) = 1 with several different values for inertial coupling (ρ) (b) Stiffness coupling(τ) = 0.175 and mass (m) = stiffness (k) = oscillator mass ratio (γ) = 1 with several different values for spring stiffness ratio (α).

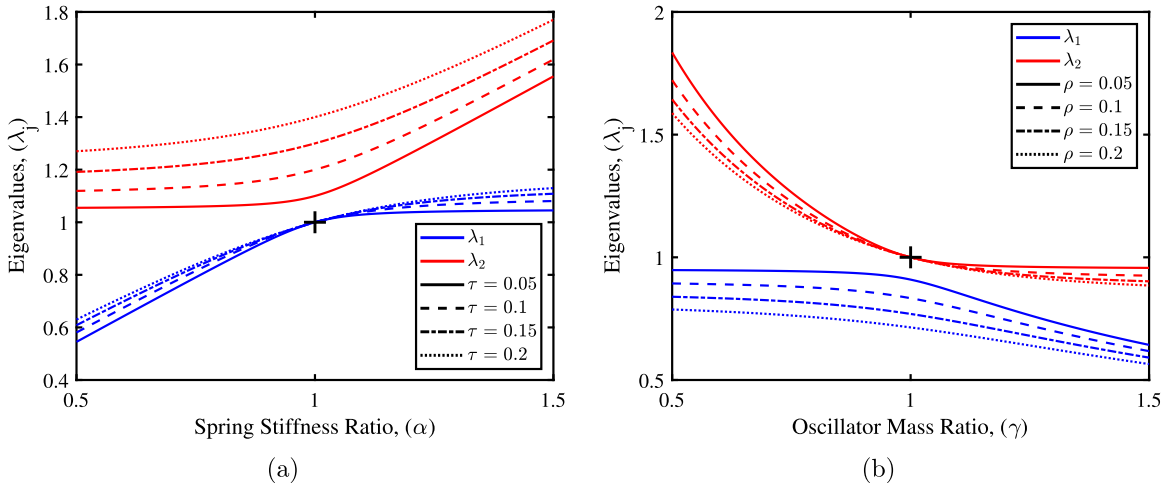

Fig. 9. Mode veering for pure coupling with the system's point of symmetry highlighted by the black cross. When α, γ, ρ or τ are varied, one eigenvalue loci curve always intersects the point of symmetry. (a) Inertial coupling (ρ) = 0 and mass (m) = stiffness (k) = oscillator mass ratio (γ) = 1 with several different values for stiffness coupling (τ) (b) Stiffness coupling (τ) = 0 and mass (m) = stiffness (k) = spring stiffness ratio (α) = 1 with several different values for inertial coupling (ρ).

7. Conclusions

This paper presents a rigorous mathematical analysis of mode veering in coupled oscillator systems with inertial coupling, implemented through an inertial amplifier. An inertial amplifier was added to a coupled double oscillator system between the two oscillating masses, both alongside and in place of a connecting spring. Using the Lagrange method and hyperbolic transformation techniques, the equations of motion for a coupled double oscillator system with both pure inertial coupling and combined inertial-stiffness coupling configurations were derived and analysed. Through systematic eigenvalue analysis, it is demonstrated that mode veering occurs in all cases except when the normalised inertial and stiffness coupling parameters are equal. This special case was proven to represent the system's point of symmetry, where the eigenvalues become non-distinct. The mathematical framework developed here establishes the fundamental relationship between coupling types, system symmetry, and mode veering behaviour. The key novel contributions of this work are:

- The first mathematical proof of mode veering in mechanically inertial-coupled systems, expanding beyond the traditional stiffness coupling domain.

- The discovery that significant mode veering can be achieved at high coupling stiffness when combined with inertial coupling of similar magnitude, a characteristic previously unattainable in pure stiffness-coupled systems.
- The identification and mathematical characterisation of the system's point of symmetry, which provides a unified framework for understanding eigenvalue behaviour in both pure and combined coupling scenarios.
- The analytical approach developed here, particularly the extension of hyperbolic transformation methods to inertial coupling, provides a robust mathematical foundation for analysing more complex coupled systems.

These findings have significant implications for the design and control of multi-degree-of-freedom mechanical systems, particularly in emerging applications such as vibration control systems, and energy harvesting devices. The ability to induce mode veering through inertial coupling, even in the absence of any stiffness coupling, offers new avenues for frequency control that were not previously available with traditional stiffness coupling approaches. Future work should focus on extending this analysis to systems with multiple degrees of freedom. Additionally, the interaction between inertial coupling and other coupling mechanisms, such as gyroscopic coupling, warrants further investigation for applications in rotating machinery and aerospace systems.

CRediT authorship contribution statement

Andrew Jacques: Writing – original draft, Visualization, Investigation, Formal analysis. **Sondipon Adhikari:** Writing – review & editing, Supervision, Software, Resources.

Declaration of competing interest

The authors declare that they have no known competing financial interests or personal relationships that could have appeared to influence the work reported in this paper.

Acknowledgements

The first author gratefully acknowledges the financial support provided by a PhD scholarship from the University of Glasgow's James Watt School of Engineering. This research was conducted using the facilities at the University of Glasgow.

Data availability

No data was used for the research described in the article.

References

[1] C. Shi, R.G. Parker, Vibration modes and natural frequency veering in three-dimensional, cyclically symmetric centrifugal pendulum vibration absorber systems, J. Vib. Acoust. 136 (1) (2014) 011014.
[2] C. Pierre, Mode localization and eigenvalue loci veering phenomena in disordered structures, J. Sound Vib. 126 (3) (1988) 485–502.
[3] A.Z. Hajjaj, N. Alcheikh, M.I. Younis, The static and dynamic behaviour of MEMS arch resonators near veering and the impact of initial shapes, Int. J. Nonlinear Mech. 95 (2017) 277–286.
[4] J.L. du Bois, S. Adhikari, N.A.J. Lieven, Eigenvalue curve veering in stressed structures: An experimental study, J. Sound Vib. 322 (2009) 1117–1124.
[5] V. Gattulli, M. Lepidi, Localization and veering in the dynamics of cable-stayed bridges, Comput. Struct. 85 (2007) 1661–1678.
[6] I. Lopez, R.R.J.J. van Doorn, R. van der Steen, N.B. Roozen, H. Nijmeijer, Frequency loci veering due to deformation in rotating tyres, J. Sound Vib. 324 (2009) 622–639.
[7] B. Mace, E. Manconi, Mode veering in weakly coupled systems, in: International Conference on Noise and Vibration Engineering, 2012, pp. 3225–3236.
[8] B. Mace, E. Manconi, Veering and strong coupling effects in structural dynamics, J. Vib. Acoust. 139 (2) (2017) 021009.
[9] J. Lin, R.G. Parker, Natural frequency veering in planetary gears, Mech. Struct. Mach. 29 (4) (2001) 411–429.
[10] C. Rosso, E. Bonisoli, F. Bruzzone, Could the Veering Phenomenon be a Mechanical Design Instrument? in: Topics in Modal Analysis and Testing, vol. 10, Soc. Exp. Mech., 2012, pp. 85–95.
[11] S.K. Singh, R.K. Varma, A. Banerjee, K.K. Rathore, Study of wave motion on the emergence of veering, locking, and coupling in periodic composite panels, J. Acoust. Soc. Am. 155 (2) (2024) 826–836.
[12] D. Fourie, R. Frohling, S. Heyns, Railhead corrugation resulting from mode-coupling instability in the presence of veering modes, Tribol. Int. 152 (2020) 106499.
[13] G. Liu, D. Gong, J. Zhou, L. Ren, Z. Wang, X. Deng, W. Sun, T. You, Frequency veering of railway vehicle systems and its mapping to vibration characteristics, Multibody Syst. Dyn. (2024).
[14] G. Dao, S. Youhong, L. Guangyu, W. Zegen, D. Xin, S. Weiguang, W. Qiushi, W. Tengfei, J. Yuanjin, Z. Kai, Z. Jinsong, Frequency veering between car body and under-chassis equipment of railway vehicles in vertical bending mode, Mech. Syst. Signal Process. 185 (2023) 109768.
[15] H. She, C. Li, Q. Tang, B. Wen, Veering and merging analysis of nonlinear resonance frequencies of an assembly bladed disk system, J. Sound Vib. 493 (2021) 114818.
[16] F. Benedettini, D. Zulli, A. Rocco, Frequency-Veering and Mode Hybridization in Arch Bridges, in: Topics in Modal Analysis and Testing, vol. 27, Soc. Exp. Mech., 2009.
[17] H. Zhang, H. Yuan, T. Zhao, Study on localization influences of frequency veering on vibration of mistuned bladed disk, J. Mech. Sci. Technol. 31 (11) (2017) 5173–5184.
[18] R. Longman, P. Hagedorn, A. Beck, Stabilization due to gyroscopic coupling in dual-spin satellites subject to gravitational torques, Celest. Mech. Dyn. Astron. 25 (4) (1981) 353–373.
[19] J.V. Pushpangathan, M.S. Bhat, K. Harikumar, Effects of gyroscopic coupling and countertorque in a fixed-Wing nano air vehicle, J. Aircr. 55 (1) (2018) 239–250.

[20] A. Gajo, The effects of inertial coupling in the interpretation of dynamic soil tests, Geotechnique 46 (2) (1996) 245–257.
[21] F.B. Usabiaga, R. Delgado-Buscalioni, B.E. Griffith, A. Donev, Inertial coupling method for particles in an incompressible fluctuating fluid, Comput. Methods Appl. Mech. Engrg. 269 (2014) 139–172.
[22] F.B. Usabiaga, I. Pagonabarraga, R. Delgado-Buscalioni, Inertial coupling for point particle fluctuating hydrodynamics, J. Comput. Phys. 235 (2013) 701–722.
[23] W.C. Verloop, The inertial coupling force, Int. J. Multiph. Flow. 21 (5) (1995) 929–933.
[24] J.A.T. Bye, Inertial coupling of fluids with large density contrast, Phys. Lett. A 202 (1995) 222–224.
[25] M. He, J. Macdonald, Aeroelastic stability of a 3DOF system based on quasi-steady theory with reference to inertial coupling, J. Wind Eng. Ind. Aerodyn. 171 (2017) 319–329.
[26] S. Vidoli, F. Vestroni, Veering phenomena in systems with gyroscopic coupling, J. Appl. Mech. 72 (5) (2005) 641–647.
[27] S. Adhikari, Inertial amplifier configurations for vibration control and mitigation, Int. J. Mech. Sci. (2022) 1–31.
[28] N.M.M. Frandsen, O.R. Bilal, M.I. Hussein, Inertial amplification of continuous structures: Large band gaps from small masses, J. Appl. Phys. 119 (12) (2016) 124902.
[29] S. Taniker, C. Yilmaz, Phononic gaps induced by inertial amplification in BCC and FCC lattices, Phys. Lett. A 377 (2013) 1930–1936.
[30] C. Yilmaz, G.M. Hulbert, N. Kikuchi, Phononic band gaps induced by inertial amplification in periodic media, Phys. Rev. B 76 (2007) 054309.
[31] M.I. Hussein, I. Patrick, A. Banerjee, S. Adhikari, Metadamping in inertially amplified metamaterials: Trade-off between spatial attenuation and temporal attenuation, J. Sound Vib. 531 (2022) 116977.
[32] S. Adhikari, A. Banerjee, Enhanced low-frequency vibration energy harvesting with inertial amplifiers, J. Intell. Mater. Syst. Struct. 33 (6) (2021).
[33] X. Kang, X. Wang, Q. Lei, G. Xia, C. Wang, Simultaneous vibration isolation and energy harvesting via a new negative stiffness system with inertial amplifier, J. Eng. Res. (2024) http://dx.doi.org/10.1016/j.jer.2024.04.012.
[34] I. Zeimpekis, I. Sari, M. Kraft, Characterization of a mechanical motion amplifier applied to a MEMS accelerometer, J. Microelectromech. Syst. 21 (5) (2012) 1032–1042.
[35] S. Chowdhury, A. Banerjee, S. Adhikari, Optimal negative stiffness inertial-amplifier-base-isolators: exact closed-form expressions, Int. J. Mech. Sci. 218 (2022) 107044.
[36] S. Chowdhury, A. Banerjee, S. Adhikari, Enhanced seismic base isolation using inertial amplifiers, Structures 3 (2021) 1340–1353.
[37] X. Kang, X. Wang, A. Zhang, G. Xia, Low frequency vibration energy harvesting of piezoelectric vibration systems with an adjustable device and inertial amplifier device, J. Vib. Eng. Technol. (2024) http://dx.doi.org/10.1007/s42417-024-01442-9.
[38] W. Zhang, W. Zhang, X. Guo, Vertical vibration control using nonlinear energy sink with inertial amplifier, Appl. Math. Mech. 44 (10) (2023) 1721–1738.
[39] S. Chowdhury, A. Banerjee, S. Adhikari, The optimal design of dynamic systems with negative stiffness inertial amplifier tuned mass dampers, Appl. Math. Model. 114 (2023) 694–721.
[40] S. Chowdhury, A. Banerjee, The impacting vibration absorbers, Appl. Math. Model. 127 (2024) 454–505.
[41] A. Banerjee, S. Adhikari, M.I. Hussein, Inertial amplification band-gap generation by coupling a levered mass with a locally resonant mass, Int. J. Mech. Sci. 207 (2021) 106630.
[42] S. Chowdhury, A. Banerjee, The nonlinear dynamic analysis of optimum nonlinear inertial amplifier base isolators for vibration isolation, Nonlinear Dynam. 111 (2023) 12749–12786.
[43] S. Chowdhury, A. Banerjee, S. Adhikari, The optimum inertial amplifier tuned mass dampers for nonlinear dynamic systems, Int. J. Appl. Mech. 15 (2) (2023) 2350009.
[44] Z. Cheng, A. Palermo, Z. Shi, A. Marzani, Enhanced tuned mass damper using an inertial amplification mechanism, J. Sound Vib. 475 (2020) 114267.
[45] R.S. Kattimani, P.V. Malaji, S.S. Chappar, S. Adhikari, Enhanced vibration energy harvesting from coupled pendulums through inertial amplifiers, Smart Mater. Struct. 33 (10) (2024) 10LT01.
[46] C. Du, Q. Cheng, K. Li, Y. Yu, Self-sustained collective motion of two joint liquid crystal elastomer spring oscillator powered by steady illumination, Micromachines 13 (2) (2022) 271.
[47] B. Balachandran, T. Breunung, G.D. Acar, A. Alofi, J.A. Yorke, Dynamics of circular oscillator arrays subjected to noise, Nonlinear Dynam. 108 (2022) 1–14.
[48] J. Chen, T. Tsukamoto, S. Tanaka, Triple mass resonator for electrostatic quality factor tuning, J. Microelectromech. Syst. 31 (2) (2022) 194–203.
[49] S. Mo, L. Wang, M. Liu, Q. Hu, H. Bao, G. Cen, Y. Huang, Study of the time-varying mesh stiffness of two-stage planetary gear train considering tooth surface wear, J. Mech. Eng. Sci. 238 (1) (2024) 279–297.
[50] Y. Li, N. Challamel, I. Elishakoff, Effective mass and effective stiffness of finite and infinite metamaterial lattices, Arch. Appl. Mech. 93 (2023) 301–321.
[51] N.G. Stephen, On veering of eigenvalue loci, J. Vib. Acoust. 131 (2009) 054501.
[52] M. Gitterman, The Chaotic Pendulum, World Scientific Publishing Company Ltd, 2010.
[53] G.L. Baker, J.A. Blackburn, The Pendulum: A Case Study in Physics, Oxford University Press, 2005.
[54] P.S. Nair, S. Durvasula, On quasi-degeneracies in plate vibration problems, Int. J. Mech. Sci. 15 (1973) 975–986.
[55] P.-T. Chen, J.H. Ginsberg, On the relationship between veering of eigenvalue loci and parameter sensitivity of eigenfunctions, J. Vib. Acoust. 114 (2) (1992) 141–148.
[56] J.J. Webster, Free vibrations of rectangular curved panels, Int. J. Mech. Sci. 10 (1968) 571–582.